Food & Function

ROYAL SOCIETY OF CHEMISTRY

PAPER

View Article Online
View Journal | View Issue

Cite this: *Food Funct.*, 2024, **15**, 2587

Structural characterisation of deer sinew peptides as calcium carriers, their promotion of MC3T3-E1 cell proliferation and their effect on bone deposition in mice†

Li Sun, [a] Jinze Liu,[a] Hongyan Pei, [a] Meiling Shi,[a] Weijia Chen,[a] Ying Zong,[a] Yan Zhao,[a] Jianming Li,[a] Rui Du *[a,b] and Zhongmei He *[a,b]

Deer sinew as a by-product has high collagen and nutritional value. This study focuses on its hydrolysate being used as a calcium carrier to develop functional foods. The chelation mechanism was analyzed by SEM, EDS, UV-vis, FTIR, and fluorescence spectroscopy and zeta potential analysis after using peptide-sequenced deer sinew peptides for chelation with calcium ions. The results showed that the chelation of deer sinew peptides with calcium ions occurs mainly at the O and N atoms of carboxyl, amino and amide bonds. *In vitro* and *in vivo* studies revealed that deer sinew peptide–calcium chelate (DSPs-Ca) promoted the proliferation of MC3T3-E1 cells without toxic side effects and increased the alkaline phosphatase activity. The DSPs-Ca group improved the bone microstructure induced by low calcium, as well as up-regulated the expression of genes responsible for calcium uptake in the kidneys, as evidenced by serum markers, bone sections, bone parameters, and gene expression analyses in low-calcium-fed mice. From the above, it can be concluded that DSPs-Ca is expected to be a calcium supplement food for promoting bone health.

Received 24th October 2023,
Accepted 6th January 2024

DOI: 10.1039/d3fo04627c

rsc.li/food-function

1. Introduction

Calcium is an important part of the human body and mainly plays a role in supporting the body, forming the skeleton, protecting the internal organs, and enzyme activation.[1] It is necessary for the biological material that forms bones.[2] Inadequate calcium intake can lead to a variety of diseases that cause many discomforts to the body, including rickets,[3] growth retardation, and a host of problems such as fractures and osteoporosis.[4] However, the current situation of inadequate calcium intake is widespread.[5] Inadequate calcium intake has been reported in studies of calcium intake in Spanish children[6] and micronutrient intake in the diets of adolescents and young children in the Netherlands.[7] An IOF (International Osteoporosis Foundation) Global Map study of the adult dietary calcium intake shows that low calcium intake is a major problem in many parts of the world, negatively affecting the health of bone tissue in populations. Bone loss accelerates in later life, and the elderly Singaporeans in the study also had inadequate calcium intake.[8] The amount of calcium needed for optimal bone health changes at different stages of life, with the need for calcium being higher in adolescence as bones grow rapidly and the body's ability to absorb calcium decreasing at older ages.[9] From the above, it can be seen that calcium plays an essential role in bone health at all ages.[10]

It is noteworthy that dietary calcium intake is usually secure and that food intake is the only way for the body to replenish calcium reserves in the bones.[11] For this reason, proper oral calcium supplementation is essential for maintaining bone health.[12] Calcium supplements mainly include inorganic calcium, organic calcium, amino acid calcium and calcium-binding peptides. Although the first three types of calcium supplements have some calcium replenishment effect, the problems of strong irritation and related adverse reactions have not been effectively solved. For example, inorganic calcium has poor solubility and is not easily absorbed. Excessive intake of organic calcium can easily cause toxic side effects.[13] Amino acid calcium is more advantageous in terms of solubility and absorption rate.[14] However, it is expensive

[a]*College of Chinese Medicinal Materials, Jilin Agricultural University, Changchun 130118, China*
[b]*Jilin Provincial Engineering Research Centre for Efficient Breeding and Product Development of Sika Deer, Changchun 130118, China. E-mail: durui@jlau.edu.cn*

† Electronic supplementary information (ESI) available. See DOI: https://doi.org/10.1039/d3fo04627c

and easily causes fat oxidation, which limit its wide application to a certain extent. In recent years, calcium-binding peptides have been isolated and characterized with great potential to promote calcium absorption.[15] This kind of calcium-binding peptide is a new direction in the development of calcium preparations. Compared with other calcium supplements, peptides in chelates not only provide a variety of biological benefits, but also their absorption has the characteristics of low energy consumption, low carrier saturation and fast absorption rate, such as zein peptides,[16] pig bone collagen peptides,[17] and others. Additionally, peptides have more abundant calcium binding sites, and the resulting complex structure is more stable. It has been reported in the literature that it can enhance intestinal calcium absorption by preventing calcium precipitation in the intestine. The reaction product can be stabilized in the gastrointestinal tract, thus enhancing bioavailability in the organism.[18] Therefore, peptide–calcium chelates can be used as a new type of nutritional supplement that can not only promote calcium absorption, but also provide functional active peptides to the consumer, playing a dual role.[19]

The development of deer products as food and dietary supplements has gained attention over the past decade or so. Among these products, consumption of venison has increased due to its unique flavor, resulting in a large amount of by-products from slaughterhouses. Compared to venison, deer sinew is an underutilised by-product of muscle stripping from deer limbs. However, deer sinew (DS) is rich in a variety of amino acids and inorganic elements and has the potential to be utilised for the production of high-value products.[20] Its collagen content is rich, higher than that of fish skin (21.6%–21.95%), pig skin (46%) and so on. Deer sinew collagen hydrolysates, deer sinew peptides (DSPs), are commonly used in dietary supplements and nutraceuticals.[21] At present, deer sinew peptides have been shown to have anti-osteoporosis activity.[22] However, it is not clear whether DSPs can be used as high-quality peptide raw materials for the preparation of peptide–calcium chelates with some ability to promote calcium absorption. Therefore, this experiment was analysed using Nano LC-MS/MS and it was found that DSPs had suitable molecular weights and a variety of essential amino acids, which determined that they could be used as high-quality peptide raw materials for the preparation of peptide–calcium chelates. Subsequently, the structure and functional characteristics of the structure were studied. Structural characterization was used to analyze whether new substances were formed, that is whether calcium and peptide were chelated successfully. Calcium binding sites were also analyzed. To demonstrate whether it can be used as a safe functional food calcium supplement through *in vivo* acute toxicity tests and *in vitro* cellular tests. Finally, the effects of the deer sinew peptide–calcium chelate (DSPs-Ca) on renal reabsorption and bone deposition of calcium were evaluated in low-calcium mice. It is expected that DSPs-Ca can be used as a safe and functional calcium supplement with great potential to ameliorate insufficient calcium intake and the resulting bone diseases.

2. Materials and methods

2.1. Materials

DSPs were produced in our laboratory. The chemicals and solvents used in this study were of analytical grade.

2.2. Peptide sequence identification

DSPs were first solubilized with 50 mM NH_4HCO_3, and then the samples were reduced, alkylated, and desalted according to a slight modification of the method described by Wang *et al.*[23] Afterwards, the treated samples were analyzed by Nano LC-MS/MS. Nanoflow UPLC: Easy-nLC 1200 system (Thermo Fisher Scientific, USA); nanocolumn: 150 μm × 15 cm in-house made column packed with Acclaim PepMap RPLC C18 (3 μm, 100 Å, Dr Maisch GmbH, Germany); mobile phase: A: 20%–0.1% formic acid in water, B: 80% acetonitrile. Total flow rate: 600 nL min^{-1}. Samples were analyzed using an Easy-nLC 1200 system coupled with a Q Exactive™ Hybrid Quadrupole-Orbitrap™ mass spectrometer (Thermo Fisher Scientific, USA) with an ESI nanospray source to analyze the samples. The raw MS files were analyzed and searched using PEAKS Studio (10.6). After *de novo* analysis, peptide sequence analysis results were obtained.

2.3. Preparation experiment of DSPs-Ca

DSPs were dissolved in ultrapure water at 5 mg mL^{-1}. Calcium chloride was added according to the peptide–calcium mass ratio of 6 : 1, and the pH was adjusted to 8 with 1 mol L^{-1} sodium hydroxide. The solution was chelated at a temperature of 55 °C for 45 min. After the calcium chelation reaction, 9 times the volume of ethanol absolute was added to precipitate the DSPs-Ca, which also served as a preliminary separation of the DSPs-Ca and calcium ions, and then the precipitate was rinsed with a 90% ethanol solution several times to remove as much as possible the free calcium ions. The precipitates were centrifuged at 4000*g* for 20 min, collected and lyophilized for further analysis.

2.4. Characterization of peptides and chelates

2.4.1. SEM and EDS of DSPs and DSPs-Ca. The DSPs and DSPs-Ca powders were sprayed with gold and placed into a scanning electron microscope (Carl Zeiss AG, ZEISS EVO 18, Germany) to evacuate the vacuum, turn on the voltage, wait for the high voltage addition to be completed, and start positioning the sample. Subsequently, the height of the sample stage to the objective was adjusted, preview parameters were set, focusing and defocusing scattering were performed, and the scanning results were waited for to obtain microstructural maps. Finally, it was photographed and saved at the set magnification and analyzed by energy dispersive spectroscopy.[24]

2.4.2. UV-vis of DSPs and DSPs-Ca. Appropriate amounts of DSPs and DSPs-Ca were prepared with ultrapure water to 1 mg mL^{-1}, respectively, and scanned at 190–400 nm. The UV-visible spectrophotometer (UV-6100, MAPADA, China) was blank-corrected with deionized water prior to the measurement of the samples. The UV absorption spectra of DSPs and

DSPs-Ca were determined by using MAPADA scanning analysis software.[25]

2.4.3. FTIR of DSPs and DSPs-Ca. The dried DSPs and DSPs-Ca (1 mg each) were taken and mixed homogeneously with an appropriate amount of KBr, pressed until transparent, and the samples were scanned using an infrared spectrometer (iS50R, Thermo Fisher Scientific, USA) over a range of 400 to 4000 cm^{-1}.[26]

2.4.4. Fluorescence spectroscopy of DSPs and DSPs-Ca. The DSPs and DSPs-Ca were briefly treated (added to deionized water and configured to 0.15 mg mL^{-1}), and a fluorescence spectrophotometer (RF6000, Shimadzu Co., Japan) was selected to measure the spectral types of emission spectra, with an excitation wavelength of 280.0 nm; the start of the emission wavelength: 290.0 nm and the end: 500.0 nm. The data interval was 1.0 nm, and the scanning speed was 600 nm min^{-1}.[27]

2.4.5. Zeta potential of DSPs and DSPs-Ca. DSPs and DSPs-Ca were prepared as 1 mg mL^{-1} solutions, respectively, and the potentials were determined using a zeta potential analyzer (90Plus Zeta, Brookhaven Instruments Co., USA).[28]

2.5. MC3T3-E1 cell proliferation assay

MC3T3-E1 cells were cultured in α-MEM supplemented with 10% fetal bovine serum. The logarithmic phase growth cells were selected, and the cell suspension was mixed and inoculated in 96-well plates at a density of about 1×10^4 cells per mL in 100 μL of cell suspension per well. After culture for 24 h, the culture medium was changed and DSPs-Ca solution with a different concentration was added. After culture for 24 h, 10 μL of CCK-8 reagent was added to each well. After continuing in the incubator for 1 h, the absorbance value was measured at 595 nm to calculate the cell viability. The evaluation of alkaline phosphatase (ALP) activity was chosen to detect ALP activity at 510 nm on days 1, 4 and 7.

2.6. Animals

2.6.1 Acute toxicity study. All animal procedures were performed in accordance with the Guidelines for Care and Use of Laboratory Animals of Jilin Agricultural University, and approved by the Animal Welfare and Ethics Committee of Jilin Agricultural University. Animal experiment ethical number: 20211011003, bought from Changchunshi Yisi Experimental Animal Technology Limited. ICR mice were selected for the study. They were allowed to acclimatize for 1 week, fed normally, with good ventilation, appropriate temperature (room temperature of 20–26 °C), and relative humidity maintained at 50%–70%. Healthy animals were segregated on the basis of difference in body weight and randomly divided into two groups of 10 animals (5 males and 5 females) each. After administration of DSPs-Ca (0, 10 g kg^{-1}), the animals were closely observed for 4 hours. The dose is based on the National Standard for Food Safety (GB 15193.3-2014). Mortality and general behavioural changes were recorded for 14 consecutive days. At the end of the treatment, the main internal organs were observed visually and the body weights and organ coefficients were recorded.

2.6.2 Animal feeding and grouping design. ICR mice SPF grade, similar weight (±10%), around 25 g, 50, male. These 50 mice were grouped: blank control group (NC), low-calcium model group (LC), deer sinew peptide-calcium chelate high-dose group (DSPs-Ca-H), deer sinew peptide-calcium chelate low-dose group (DSPs-Ca-L), and calcium chloride group (CC). The NC group was fed a conventional diet (calcium mass fraction – 0.5%) and the rest of the groups were fed a low calcium diet (calcium mass fraction – 0.05%). Calcium intake in the high and low dose groups was referenced to 10 and 5 times the recommended daily intake of 800 mg per 60 kg for humans, and the gavage dose was based on calcium content. Fig. 1 illustrates the experimental design protocol, including the feeding method, gavage dose, and overall tissue of each group of mice.

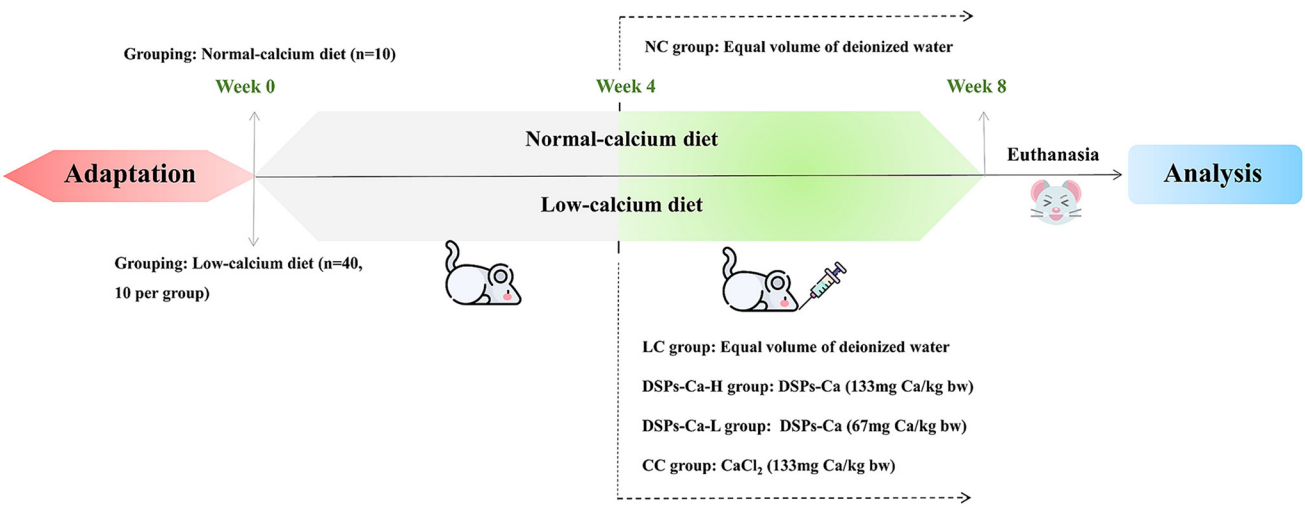

Fig. 1 Experimental design of the animal study.

2.6.3. Sample collection and methodology. The body weights of the mice were recorded during the four weeks when gavage was initiated. After eight weeks, all mice were fasted for 12 h and blood was collected for measurement of serum calcium, phosphorus and alkaline phosphatase (ALP) levels. The mice were euthanized and the hearts, livers, spleens, lungs, kidneys, and femurs were quickly removed and stored at −80 °C for further analysis. Femur length was measured using vernier calipers. Visceral index was calculated (visceral index (100%) = visceral weight/body weight).

The dry weight of the femur was recorded after baking the left femur of mice in an oven until constant weight. The femur, which was baked to constant weight, was mashed and transferred to a conical flask with 10 mL of mixed acid (nitric acid : perchloric acid = 4 : 1, v/v). It was placed in a digestion oven, warmed up and digested until transparent, and then the content of bone calcium was determined by atomic absorption spectrometry (AA-6300F/G, Shimadzu Co., Japan).

2.6.4. Hematoxylin–eosin (HE) staining of femur. Paraffin sections were made from mouse femurs, and HE staining was performed according to the routine procedure, in which the paraffin sections were sequentially placed in xylene and alcohol and deparaffinized to water. The sections were placed in a hematoxylin staining solution for 3 to 5 minutes, followed by a hematoxylin differentiation solution for a few seconds, and finally placed in hematoxylin anti-blue solution to re-bleach the blue, and each step involved rinsing with tap water. The sections were then stained with eosin staining solution for 5 minutes, followed by dehydration, attaining transparency, sealing, microscopic observation, and photographing.

2.6.5. Micro-computed tomography (micro-CT) analysis. Femur specimens from each group of mice were taken and the surrounding tissue was cleaned off, and then fixed in 4% paraformaldehyde for 24 h. Micro CT (Siemens Inveon Micro CT, SIEMENS AG, Germany) analysis was performed, and the scanning parameters were set as: a voltage of 80 kV, a current of 500 μA, the average number of frames of 1, and a bin factor of 1. The scanning rotation angle was 360° and the number of scanning steps was 180 steps. Scanning was also performed using the Inveon Acquisition Workplace system that came with the machine to obtain micro CT images with a reconstruction scale factor of 2.

2.6.6. Quantitative real-time PCR. Total RNA from mouse kidneys was extracted using TRIzol (Invitrogen, USA). At the end of the extraction reaction, reverse transcription was performed using the RevertAid First Strand cDNA Synthesis Kit with oligo-dT as the primer. The cDNA target sequences were determined on a real-time PCR instrument (Roche LightCycler 480II, USA) using a QuantiTect SYBR Green RT-PCR Kit. The β-actin internal reference gene was selected for correction and normalization, and the mRNA expression of the gene in kidney tissue was calculated using the $2^{-\Delta\Delta Ct}$ method. Primer sequences can be found in Table S1.†

2.7. Statistical analysis

All the above data were statistically analyzed using SPSS 26.0 software. Data are expressed as mean ± standard deviation (mean ± SD). Data were analyzed by one-way analysis of variance (ANOVA) with Tukey's test. Differences were considered statistically significant when $P < 0.05$. Meanwhile, Origin 2022 was selected for graphical visualization.

3. Results and discussion

3.1. Peptide sequence analysis

Studies have shown that the chelating ability of peptides has a correlation with molecular weight, sequence and amino acid composition.[19] Thus, the sequence of DSPs was determined by Nano LC-MS/MS and the total ion flow chromatogram was obtained (Fig. 2). Table 1 shows the top 10 peptides with a

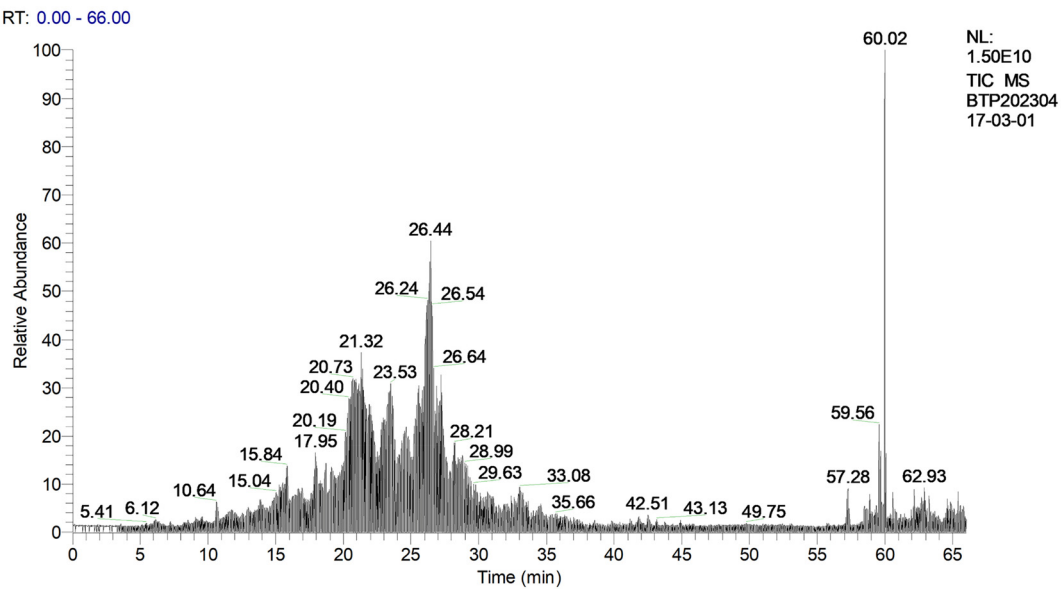

Fig. 2 Total ion flow chromatography of DSPs.

Table 1 Top 10 peptides with higher *de novo* score for DSPs

Sequence	*De novo* score	Mass (Da)	Structural formula
KDGRPGPLGPA	99	1105.5879	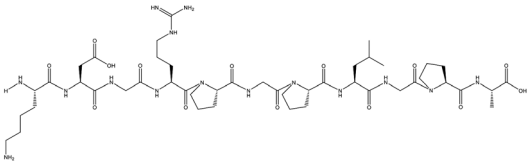
KDRGPGPLGPA	99	1105.5879	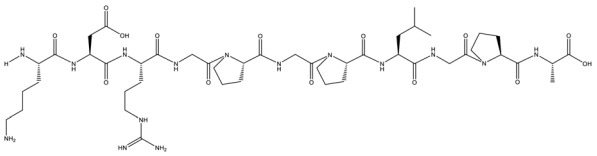
VPGPMGPSGPR	99	1050.5281	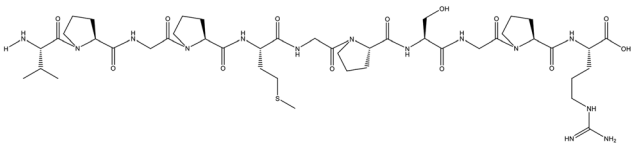
PLPEFT	99	702.3588	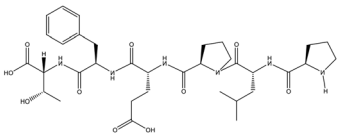
LPSPLRP	99	778.4701	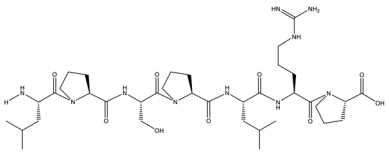
VPLPV	99	523.337	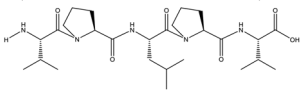
GPVGPAG	99	553.2859	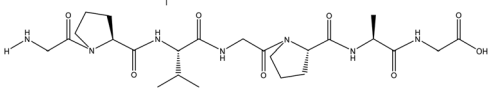
ASGPAGPR	99	711.3663	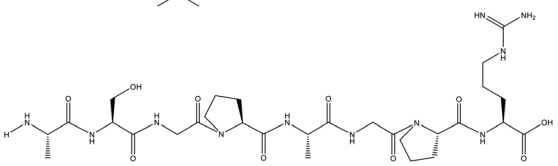
GDAGPAGPK	99	768.3766	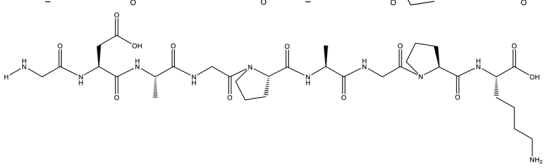
AGPAGPR	99	624.3343	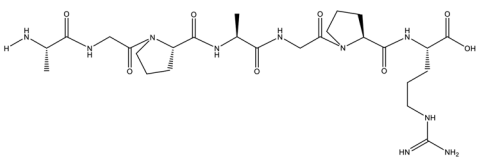

higher *de novo* score for DSPs. The list of remaining identified peptides is shown in Table S2.† And it contains 632 different peptides, with the number of amino acids in the peptides ranging from 4 to 23, and the molecular weight ranging from roughly 400 to 2300 Da. We analyzed whether DSPs can be an ideal source of calcium supplements from three aspects. First, in molecular weight distribution, as shown in Table 2, the

Table 2 The number of peptides with different molecular weights

Molecular weight range (Da)	>1500	1000–1500	500–1000	<500
Number of peptides	27	191	387	27

molecular weights of deer sinew peptides are mainly concentrated in two ranges, 500–1000 and 1000–1500 Da. It has been shown that the molecular weight distribution of peptides is critical for calcium–peptide binding, with fragments with molecular weights below 3000 Da having higher calcium binding capacity.[29] However, more small molecules (<500 Da) in the wheat germ hydrolysis products were detrimental to the calcium-binding capacity.[30] Secondly, on the peptide sequences of the DSPs, a plurality of peptides, such as VPGPMGPSGPR, GDAGPAGPK, GPAGPAGGPR, GPVGPAG, and so on, have triplet repeats of the (Gly-X-Y)n primary structure of the collagen peptide chain. Some studies have found that some collagen peptides such as those found in tilapia bones[31] and in Pacific cod skin[32] have a somewhat high affinity for calcium. Finally, in terms of amino acid composition, there is a large body of research showing that the carboxyl groups of Glu and Asp are critical to the calcium affinity of the peptide.[33] Sheep collagen peptide–calcium chelates were found to be rich in Ala, Glu, Asp and Gly.[34] The relative percentage contents of Asp, Thr, Ser and Glu increased to different degrees after the casein calcium-binding peptide was chelated with calcium,[35] suggesting that these amino acids play an important role in the chelation process with calcium. At high pH, conditions corresponding to calcium uptake with high binding affinity include Asp, Glu, Leu, His, Ala, and Gly.[36] In the sequence results of DSPs, Glu, Asp, Gly, Ala, Thr, and Ser appeared with high frequency and were present in 105, 161, 558, 442, 256, and 338 peptides, respectively. Meanwhile, the percentage of occurrences of Asp, Glu, Leu, His, Ala and Gly in these peptide sequences was 47.29%. From this, it can be inferred that there is a theoretical basis for the binding of DSPs to calcium, which can be followed up. DSPs may be a source of calcium-binding peptides in functional foods.

3.2 SEM and EDS analysis of DSPs and DSPs-Ca

The combination of a scanning electron microscope and other analytical instruments can be done to characterize the microscopic morphology and at the same time to carry out the analysis of the composition of the microregion of the substance, which is of some significance for the food field.[37] Fig. 3A and C show the microscopic morphology of DSPs and DSPs-Ca. At 10.00 k magnification, it can be observed that the deer sinew peptide shows a smooth and uniform planar surface, whereas the deer sinew peptide–calcium chelate formed with calcium ions was broken into isolated solid blocks with irregular shapes and rough and uneven surface structures. This may be due to the breaking of the original structure of the peptide after chelation, leading to structural changes in the peptide and the formation of irregular particles.[38] The EDS in Fig. 3B and D show the elemental composition of DSPs and DSPs-Ca. The DSPs contained elements such as C, N, and O with mass percentages of 43.08%, 15.71%, 25.98%, and so on. DSPs-Ca contained elements C, N, O, and Ca with mass percentages of 36.79%, 14.71%, 31.25%, and 5.2%, respectively. The diagram of DSPs-Ca appeared to have three spectral peaks for elemental calcium, which was not detected in the DSPs. In addition, the EDS showed that the mass percentages of chloride ions were close to each other (DSPs: 2.07%, DSPs-Ca: 1.93%), which can further indicate that it was the calcium ions in the introduced $CaCl_2$ reagent that bind to the deer sinew peptide, whereas the $CaCl_2$ molecules and chloride ions in the reagent were excluded, and it is the calcium ions that chelate with the deer sinew peptide and form a new substance.

3.3. UV-vis analysis for DSPs and DSPs-Ca

Ultraviolet–visible absorption spectra are generated from the valence electrons and electrons in molecular orbitals in the electronic energy levels between the transition. The use of material molecules or ions for the absorption of ultraviolet and visible light produced by the spectral absorption and the degree of absorption of the structure of the material can be analyzed, measured and deduced. When the organic ligand combines with the metal ion calcium, it causes the original absorption peak to shift or disappear or a new absorption peak to appear.[39] Therefore, the changes in the absorption wavelength and absorption intensity of the UV absorption spectrum are used to determine whether a new substance has been produced. Generally, the absorption peaks of peptide bonds in amino acid molecules are located between 200 and 300 nm. Among them, amino acid molecules containing aromatic rings – such as phenylalanine, tyrosine and tryptophan – their absorption peaks are located between 250 and 280 nm, while amino acid molecules not containing benzene rings – such as alanine and glycine – their absorption peaks are located between 200 and 220 nm.[26] As can be seen in Fig. 3E, the UV-visible spectra of DSPs and DSPs-Ca are quite different. The maximum absorption peaks of both were found between wavelengths 200 and 220 nm, and the maximum absorption peak of DSPs was 214 nm, while the maximum absorption peak of DSPs-Ca was located at 207 nm, indicating that the absorption peaks of this peptide were blue shifted after binding with calcium, which might be related to the $n \rightarrow \pi^*$ jump of C=O in the peptide bond.[40] Between the wavelengths of 250 and 280 nm, it was observed that the spectra of DSPs-Ca were flatter compared with those of DSPs, which could be attributed to the fact that the metal ions bind to some aromatic amino acids on the DSPs to form new chemical compounds, which affects the $\pi \rightarrow \pi^*$ electronic leaps of the conjugated double bonds.[41] Overall, the absorption intensity of the chelate with metal ions was higher than that of the peptide alone in the near-ultraviolet region, which may be due to the change in the chirality of the chromophore (C=O) and auxochrome (–OH, $-NH_2$) of the DSPs that chelate with the calcium ions. From the above, it can be hypothesized that the combination of DSPs with calcium resulted in chelation and the production of new compounds.

3.4. FTIR of DSPs and DSPs-Ca analysis

When metal ions bind to the organic groups of peptides, FTIR is altered and can effectively distinguish the spectral differences between peptides and their metal chelates.[42] As shown in Fig. 3F, in the 4000–2500 cm^{-1} segment (ν X–H stretching

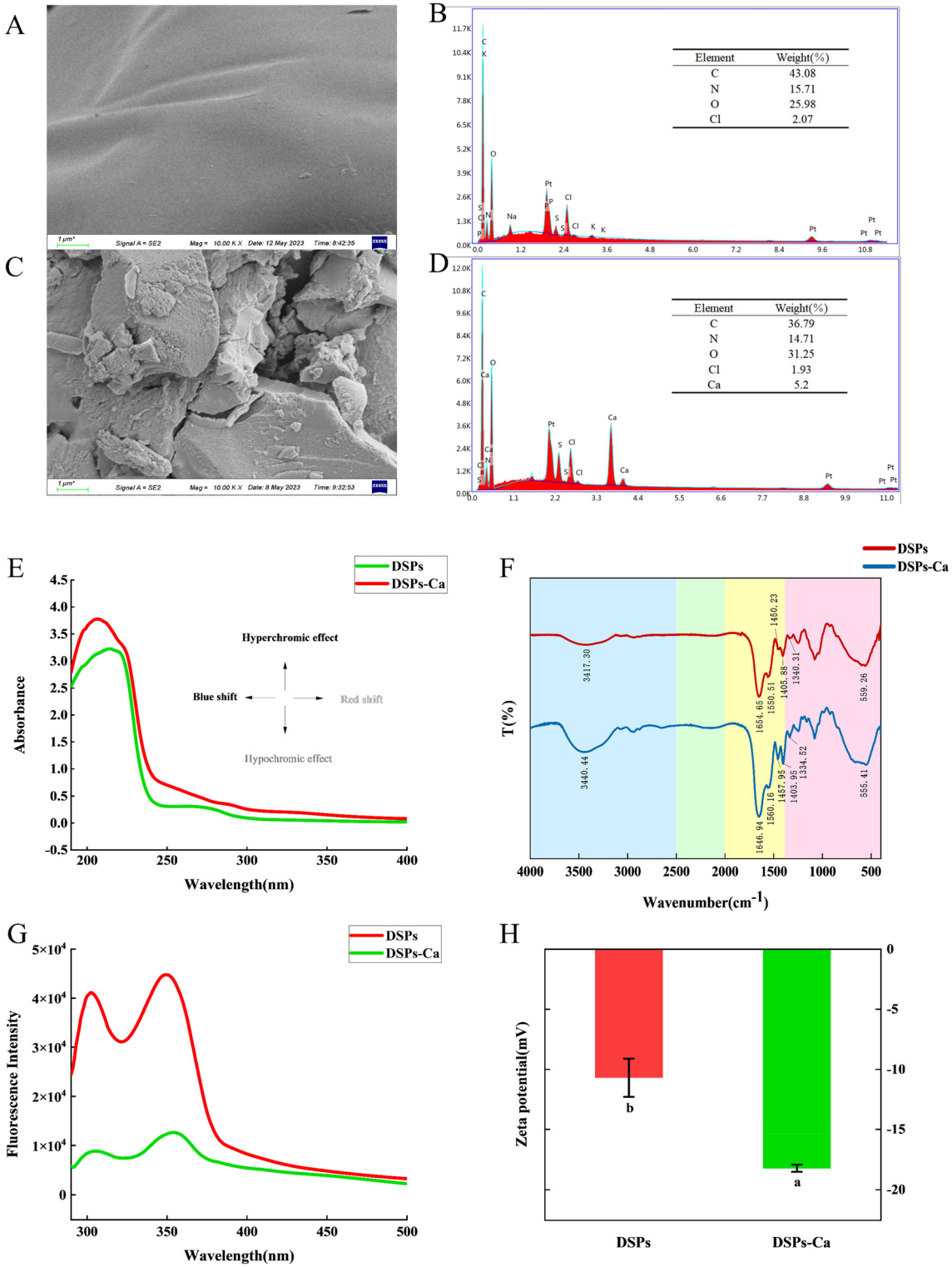

Fig. 3 SEM of (A) DSPs and (C) DSPs-Ca; EDS of (B) DSPs and (D) DSPs-Ca; (E) UV-vis, (F) FTIR, (G) fluorescence spectroscopy, and (H) zeta potential of DSPs and DSPs-Ca. Different letters indicate significant differences between the groups ($P < 0.05$).

vibration region), the stretching vibrations of N–H and O–H bonds in deer sinew peptides overlapped, and its absorption peak was shifted from 3417.30 cm^{-1} to 3440.44 cm^{-1} upon binding with calcium, which may be due to the inductive effect or the dipole field effect, and the density of the electron cloud of its N–H bond became stronger. It was speculated that the N–H bond was involved in the formation of the chelate. In the 2500–2000 cm^{-1} segment (stretching vibrational region of

triple and cumulative double bonds), there was no characteristic absorption. In the 2000–1400 cm^{-1} and 1400–400 cm^{-1} segments (the former double-bond stretching vibration region, the latter single-bond stretching vibration and the bending vibration region), it contains amide I, II and III bands, which are the important absorption regions to distinguish between DSPs and DSPs-Ca. The absorption peaks of deer sinew peptide amide bands I (C=O stretching vibration) were shifted from 1654.65 cm^{-1} to 1646.94 cm^{-1}. The absorption peaks of deer sinew peptide amide bands II and III (N–H and C–N) were shifted from 1550.51 cm^{-1} and 1340.31 cm^{-1} to 1560.16 cm^{-1} and 1334.52 cm^{-1}, which may be due to the difference in the coupling between δ NH and ν C–N affected by binding with calcium, and the peptide bond was speculated to be involved in the chelating reaction of the deer sinew peptides with Ca^{2+}.[43] In addition, the absorption peaks of the –COOH and $–COO^-$ stretching vibrations of the deer sinew peptides were shifted from 1450.23 cm^{-1} and 1405.88 cm^{-1} to 1457.95 cm^{-1} and 1403.95 cm^{-1}, which may be caused by binding with Ca. The chelation mode is mainly being due to the unbound free electrons on the carbonyl oxygen. Meanwhile, the peak of the deer sinew peptide at 559.26 cm^{-1} shifted to 555.41 cm^{-1}, which might be caused by the stretching vibration of N–Ca. It was introduced by analyzing the infrared spectra of DSPs and DSPs-Ca that carboxyl oxygen atoms and amino nitrogen atom bonds in the peptide might be involved in the chelation reaction with calcium ions to produce a new substance.

3.5. Fluorescence spectrum analysis of DSPs and DSPS-Ca

Fluorescence spectroscopy allows exploration of the interactions between organic ligands and metal ions by detecting changes in the wavelength and fluorescence intensity in the spectrum, and tracking changes in the folding or unfolding of peptides.[44] Trp, Phe, and Tyr are intrinsically fluorescent, and these three amino acids have different fluorescence excitation and emission spectra due to the differences in their side chain chromophores.[45] It can be seen from Fig. 3G that the peptide–calcium complexes formed by the chelation reaction of DSPs with calcium ions produced some changes in the position and intensity of the strongest peaks, and the intensity of the peaks of DSPs-Ca was much lower than that of the peaks of DSPs. The absorption peaks of DSPs were shifted from 303 nm and 349 nm to 305 nm and 354 nm, respectively, and the positions of the peaks corresponded exactly to the maximum emission wavelengths of about 348 nm for tryptophan and 303 for tyrosine; the fluorescence intensities of the DSPs were also decreased from 4.1×10^4 and 4.5×10^4 to 0.9×10^4 and 1.3×10^4, respectively. Since the process of chelation of calcium ions with peptides can produce endogenous fluorescence quenching and changes in their structure, it is also possible that calcium ions cause changes in the electronic structure (energy levels) of the excited state of the chromophore, which alters fluorescence intensity reduction.[46,47] Thus, these changes may be triggered by the chelation of calcium ions with peptides.

3.6. Zeta potential analysis of DSPs and DSPs-Ca

Zeta potential is a parameter for the study of electrical interactions in foods, which determines the types of particle–particle and particle–medium interactions and significantly affects sensory properties, and is used to examine food structure and stability.[28] As can be seen from Fig. 3H, the potentials of both DSPs and DSPs-Ca were negative, and the absolute value of the potentials of DSPs decreased significantly from the original −18.22 mV to −10.69 mV after binding with calcium ions ($P < 0.05$). This may be due to the negative charge of DSPs combined with positively charged calcium ions; the charge on the surface of DSPs decreased significantly, indicating that the DSPs formed a new compound with calcium ions.

3.7. Effect of DSPs-Ca on the proliferation of MC3T3-E1 cells

Based on the correlation between cellular metabolic viability and cell number, the viability level of cells was assessed by measuring their ability to reduce CCK-8 reagents. As shown in Fig. 4A, DSPs-Ca had no significant inhibitory effect on cell survival compared with the control. Instead, DSPs-Ca significantly increased the proliferative viability of MC3T3-E1 cells, indicating that it was not toxic to cell growth. And the osteoblast proliferative effect of DSPs-Ca was positively correlated with its mass concentration in the range of 50–1000 μg mL^{-1} mass concentration. Selection of DSPs-Ca had a significant effect on the proliferation of MC3T3-E1 cells, but the effect was smaller than other concentrations. DSPs-Ca of 100 μg mL^{-1} was selected to study the activity of alkaline phosphatase.

Alkaline phosphatase (ALP) is a marker enzyme secreted by osteoblasts at the early stage of differentiation and is an important indicator of their osteogenic activity, with an increase in ALP viability indicating a facilitated stage of osteoblast differentiation.[48] The results are shown in Fig. 4B. After 1 day of treatment with DSPs-Ca, there was no significant difference in ALP activity between the DSPs-Ca group and the control group ($P > 0.05$). After 4 and 7 days of incubation, there was a significant difference in ALP activity between the DSPs-Ca group and the control group ($P < 0.05$). ALP reached 12.15 ± 0.42 U mg^{-1} prot on day 7. This indicated that DSPs-Ca significantly increased osteoblast ALP viability and promoted osteoblast differentiation.

3.8. Acute toxicity study

Functional food is a type of food that has the common characteristics of general food. And it is a food that does not cause any acute harm to the human body. In order to ensure the safety of DSPs-Ca, an acute toxicity test was conducted.[49] No animals displayed any negative effects or clinical symptoms of poisoning during the study. In addition, no obvious autopsy signs, including bleeding and organ colour or size changes, were observed. The results in Table 3 show that there were no signs of lethality and mobility changes in the animals within 14 days. After 14 days of treatment, the weight changes of mice of each sex were recorded, and the results showed that the

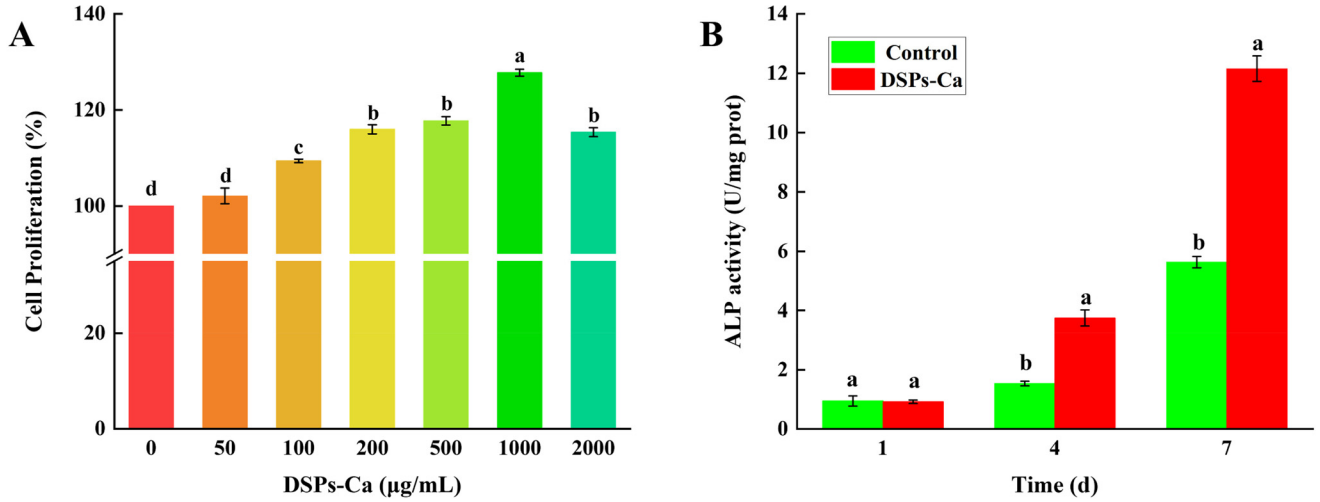

Fig. 4 Effects of DSPs-Ca on the proliferation of MC3T3-E1 cells. (A) Cell proliferation. (B) ALP activity. Different letters indicate significant differences between the groups ($P < 0.05$).

Table 3 The general behavior and body weight of mice treated with DSPs-Ca under the acute toxicity studies of the mice

Gender	Dose (g kg^{-1})	Initial weight (g)	Fourteenth day (g)	Mobility changes	Deaths
Female	0	20.16 ± 0.1748	24.70 ± 0.6835	0	0
	10	20.09 ± 0.1583	24.04 ± 0.4920	0	0
Male	0	20.48 ± 0.2867	25.53 ± 0.1383	0	0
	10	20.80 ± 0.0815	24.91 ± 0.7398	0	0

Values were expressed as mean ± SD. There were no significant differences between the groups ($P > 0.05$).

Table 4 Relative organ weights (g) of mice treated with DSPs-Ca and the control

Gender	Dose (g kg^{-1})	Heart	Liver	Spleen	Lungs	Kidneys
Female	0	0.0078 ± 0.0088	0.0339 ± 0.0344	0.0041 ± 0.0045	0.0086 ± 0.0079	0.0147 ± 0.0151
	10	0.0097 ± 0.0005	0.0363 ± 0.0020	0.0049 ± 0.0004	0.0088 ± 0.0010	0.0157 ± 0.0006
Male	0	0.0114 ± 0.0004	0.0385 ± 0.0005	0.0063 ± 0.0009	0.0106 ± 0.0004	0.0168 ± 0.0006
	10	0.0120 ± 0.0007	0.0395 ± 0.0015	0.0071 ± 0.0005	0.0117 ± 0.0010	0.0175 ± 0.0013

Values were expressed as mean ± SD. There were no significant differences between the groups ($P > 0.05$).

weight changes were not significant ($P > 0.05$), and the weight gradually increased during the whole study period. As shown in Table 4, the coefficients of the heart, liver, spleen, lungs, and kidneys were within the normal range and did not change significantly when compared to the control group ($P > 0.05$). Consequently, the NOAEL (no-observed-adverse-effect level) was considered to be 10 g kg^{-1} day^{-1}.

3.9. Body weight and visceral indices of mice

Organ coefficient is a commonly used index in toxicology experiments, and the ratio of each organ to body weight is relatively constant under normal conditions.[50] During 8 weeks, all groups of mice did not die, and there was no abnormal behavior, such as in feeding and excretion. As shown in Fig. 5A, after low-calcium modelling, there was no difference in the mean daily weight gain of each group for 4 weeks of gavage in the NC, LC, DSPs-Ca-H, DSPs-Ca-L, and CC groups ($P > 0.05$). As seen in Fig. 5B, the differences in visceral indicators of the heart, liver, spleen, lungs and kidneys were not significant in each group ($P > 0.05$). From the above analysis, it was observed that DSPs-Ca did not damage the organs of mice, did not affect the normal development of mice, and was not found to have toxic effects on mice.

3.10. Measurement of serum biochemical indices

The key biochemical indicators related to bone growth that also assess calcium absorption are serum Ca, P and alkaline phosphatase. Calcium and phosphorus play a huge role in normal physiological processes in the body, and serum calcium and phosphorus levels are closely linked and regu-

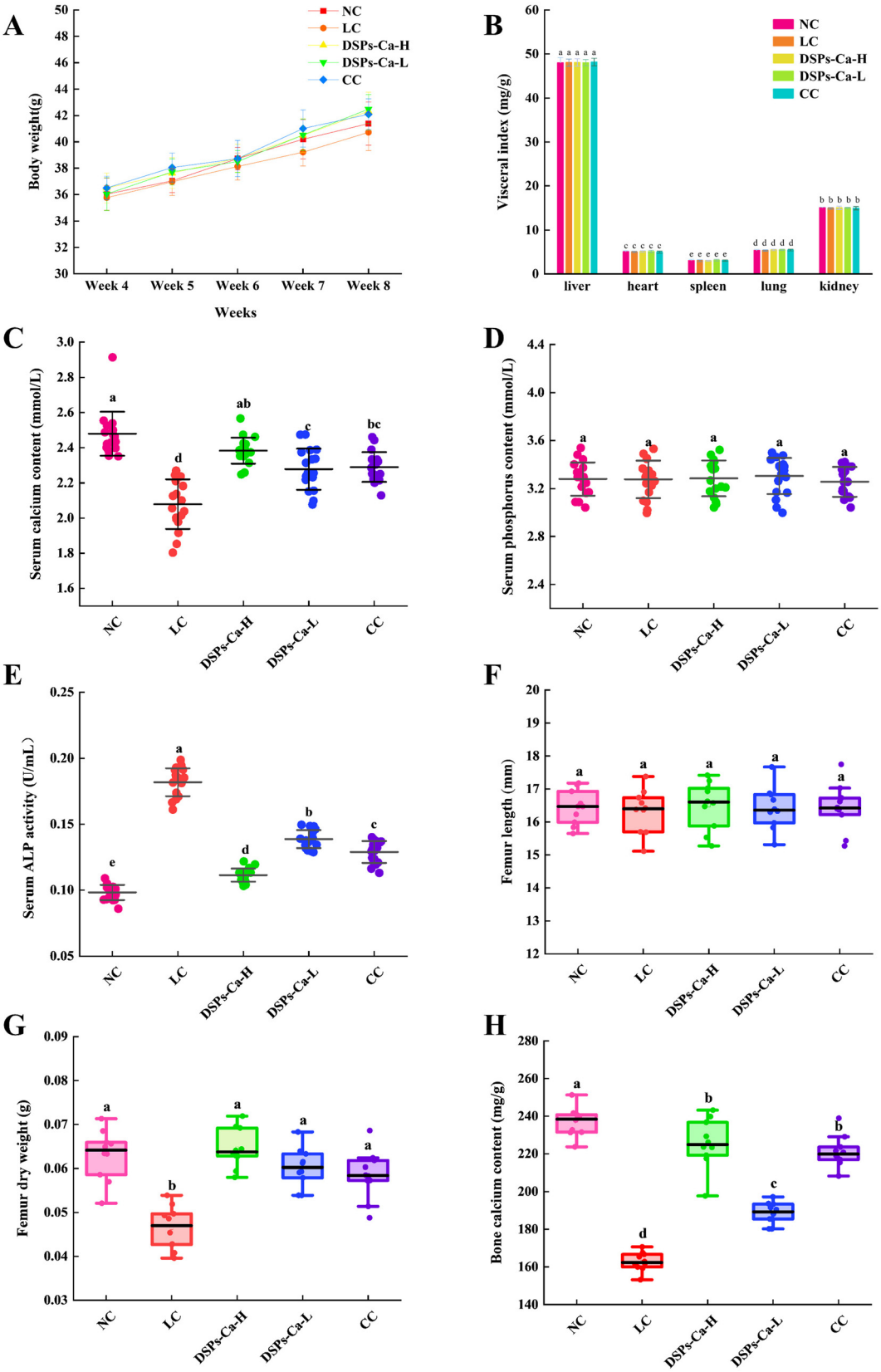

Fig. 5 (A) Body weight, (B) visceral index, (C) serum calcium content, (D) serum phosphorus content, (E) serum ALP activity, (F) femur length, (G) femur dry weight, and (H) bone calcium content of mice in the various groups. Different letters indicate significant differences between the groups ($P < 0.05$).

lated by each other. If there is an imbalance between the two, it may lead to bone disease. When the body is in a state of calcium deficiency, serum calcium levels decrease.[51] As seen in Fig. 5C, serum calcium levels were significantly decreased in the low-calcium mice ($P < 0.05$). It may be that long-term low calcium intake led to severe calcium deficiency in mice. But there was a certain degree of increase in serum calcium levels when DSPs-Ca was ingested, which proved the pro-calcium absorptive ability of DSPs-Ca. As seen in Fig. 5D, there was no significant difference ($P > 0.05$) in the serum *P* content of the mice in each group. Alkaline phosphatase (ALP) is a bone formation marker that reflects osteoblast activity and the bone formation status. ALP activity was negatively correlated with calcium intake, and the serum ALP level was significantly higher in the LC group compared with the NC group ($P < 0.05$); the DSPs-Ca-H, DSPs-Ca-L, and CC groups all reduced the serum ALP level to varying degrees compared with the LC group ($P < 0.05$), whereas the ALP level of DSPs-Ca-H was closer to that of the NC group (Fig. 5E). Therefore, DSPs-Ca could have a certain role in promoting calcium absorption.

3.11. Femoral indicators

Bone calcium content is an important indicator for evaluating bone quality. When calcium is deficient, the body's calcium balance is disrupted. Calcium is lost from the bones, impairing bone quality.[52] In order to evaluate the effectiveness of DSPs-Ca in promoting bone calcium deposition more intuitively, the femur length and femur dry weight were also measured. As can be seen from the femur length measurements in Fig. 5F, the femur lengths of the DSPs-Ca-H, DSPs-Ca-L, and CC groups were slightly longer compared to the LC group, but there was no significant difference ($P > 0.05$). It has also been shown that in most cases, the diet does not alter macrostructural characteristics such as femur length.[53] As shown in Fig. 5G and H, the femoral shaft weight and bone calcium content in the LC group were significantly lower than those in the NC group ($P < 0.05$). The femur dry weight in the DSPs-Ca-H, DSPs-Ca-L and CC groups was significantly higher than that in the LC group ($P < 0.05$), but there was no significant difference between the three groups. The bone calcium content in the DSPs-Ca-H, DSPs-Ca-L and CC groups was significantly higher than that in the LC group ($P < 0.05$), and there was no significant difference between the DSPs-Ca-H group and the CC group ($P > 0.05$). These results indicated that supplementation of DSPs-Ca could promote bone calcium absorption and calcification in the state of low calcium.

3.12. Morphological observation of bone tissue

HE staining of samples stained with hematoxylin and eosin can clearly identify the morphologic structure of tissues, which can play an auxiliary role in exploring the effects of DSPs-Ca on calcium absorption and bone deposition in mice.[54] Thus, the femur sections of the mice in each group were stained to observe the microstructure and growth of the bone. HE staining showed that the trabeculae of the bone samples in the NC group were coarse, tightly structured, neatly aligned, and had good continuity, showing a reticular distribution, whereas in the LC group, the degree of separation increased, the trabeculae were severely fractured, and the connecting interruptions of the trabeculae were markedly increased, with the trabeculae being sparsely distributed. Compared with the LC group, mice in the DSPs-Ca-H group had significantly more bone trabeculae, more connections, narrower gaps between trabeculae, and denser structures. The trabecular bone of the DSPs-Ca-L group was clear but discontinuous. The bone trabeculae of the CC group were thick, discontinuous and densely distributed (Fig. 6A). As a result, low calcium could cause changes in the structure of trabecular bones, which could be improved to varying degrees with calcium supplementation.

3.13. Micro-CT analysis

In the field of bone tissue research, micro-CT enables 2D and 3D image observations of bone morphological changes to characterize bone growth and development levels. At the same time, it is used to study the quantitative indexes and microscopic changes of bone structure and bone density, and is a powerful tool for monitoring calcium deposition in bone.[51] As shown in Fig. 6B, we can see the changes in femoral microstructure observed in micro-CT 3D/2D reconstruction images for different groups. The bone trabeculae of mice in the NC group showed a dense meshwork and their structure was intact. However, the microstructure of bone trabeculae in the mice in the LC group was altered, and their structure was severely damaged and became looser. The trabecular bone structure of mice supplemented with DSPs-Ca-H, DSPs-Ca-L and CC was improved to varying degrees.

Bone mineral density (BMD) is an essential marker of bone quality, reflecting the degree of osteoporosis and an important predictor of fracture risk.[55] As shown in Fig. 7A, the BMD of mice in the LC group was significantly lower (556.30 ± 4.21 mg cm^{-3}, $P < 0.05$) compared with that of mice in the NC group (618.23 ± 8.16 mg cm^{-3}). The BMD was 600.51 ± 3.13, 570.69 ± 4.95 and 575.72 ± 8.82 mg cm^{-3} in the DSPs-Ca-H, DSPs-Ca-L and CC groups, respectively, and was significantly higher in the DSPs-Ca-H group than in the DSPs-Ca-L and CC groups ($P < 0.05$). Although the BMD in the CC group was slightly higher than that in the DSPs-Ca-L group, there was no significant difference ($P > 0.05$). Therefore, DSPs-Ca could be more effective than $CaCO_3$ in enhancing bone mineral density and thereby improving bone quality.

Bone volume fraction (BV/TV) is a commonly used index for evaluating cancellous bone mass. For intramural cancellous bone, this ratio can reflect the trabecular bone mass of different samples. An increase in this ratio indicates that bone anabolism is greater than catabolism, resulting in an increase in bone mass, and *vice versa*. Thus, it can indirectly reflect the status of bone metabolism. The trabecular number (Tb.N), trabecular thickness (Tb.Th), and trabecular separation (Tb.Sp) were calculated from the microstructure of the trabeculae, which are the main indexes for evaluating the spatial morphology and structure of the trabeculae. When bone catabolism is greater than bone anabolism, such as in the case of

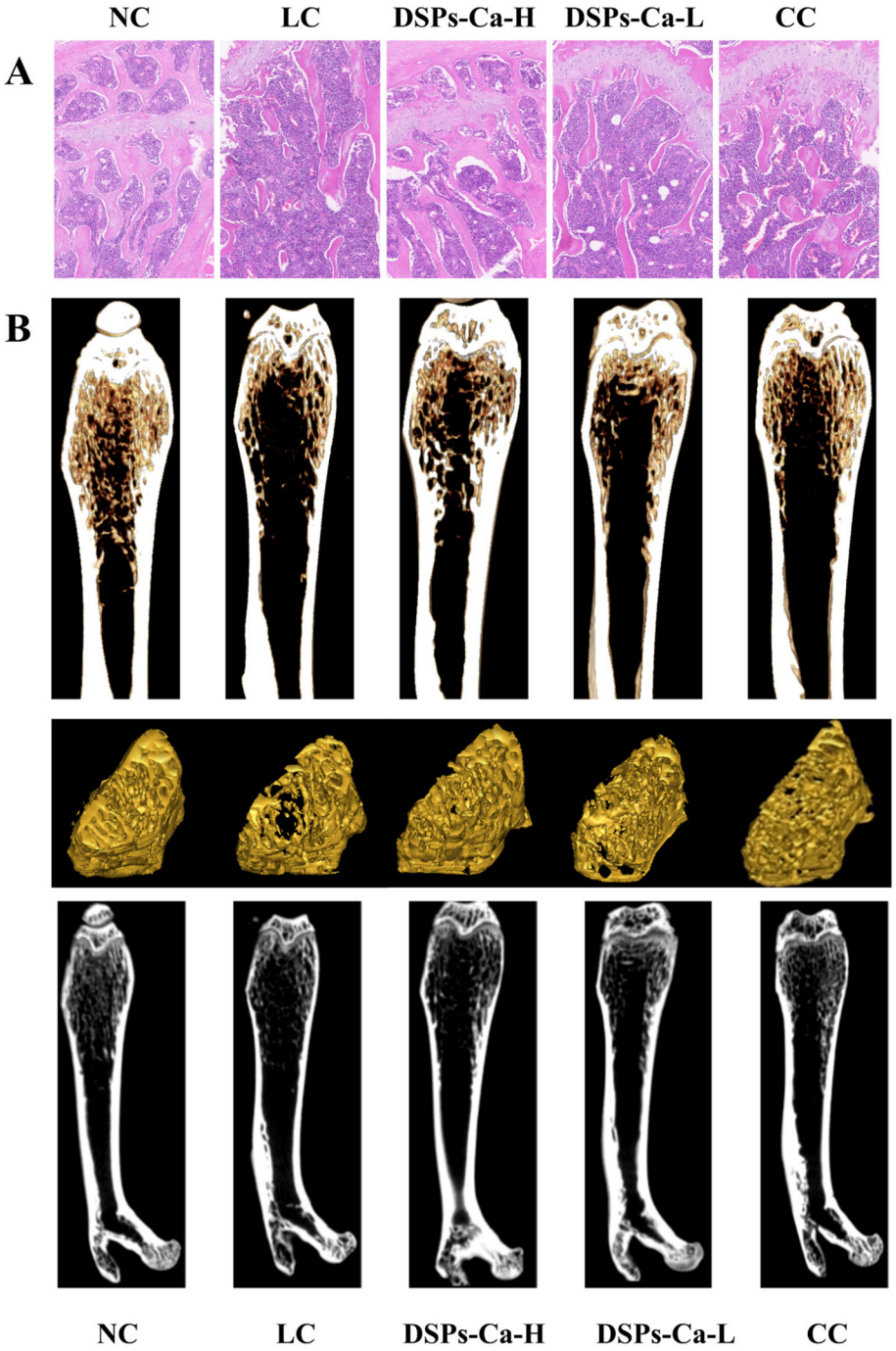

Fig. 6 (A) Morphologic observation of the bone tissue at ×100 magnification and (B) three-dimensional and two-dimensional micro-CT images of the femur in each group of mice.

osteoporosis, the values of Tb.Th and Tb.N decrease, and the value of Tb.Sp increases.[56] As shown in Fig. 7B, C and D, BV/TV, Tb.Th, and Tb.N were significantly lower in the LC group compared with the NC group ($P < 0.05$). The DSPs-Ca-H, DSPs-Ca-L and CC groups were significantly higher compared to the LC group. In addition, the values of BV/TV, Tb.Th and Tb.N were significantly higher in the DSPs-Ca-H group than in the DSPs-Ca-L and CC groups. As can be seen in Fig. 7E, Tb.Sp was significantly higher ($P < 0.05$) in mice in the LC group compared to the NC group. Those in the DSPs-Ca-H, DSPs-Ca-L and CC groups were all significantly lower compared to the LC group. In addition, the values of Tb.Sp in the DSPs-Ca-H group were significantly lower than those in the DSPs-Ca-L and CC groups. These results suggest that bone microstructural degeneration caused by calcium deficiency can be ameliorated by supplementation with DSPs-Ca.

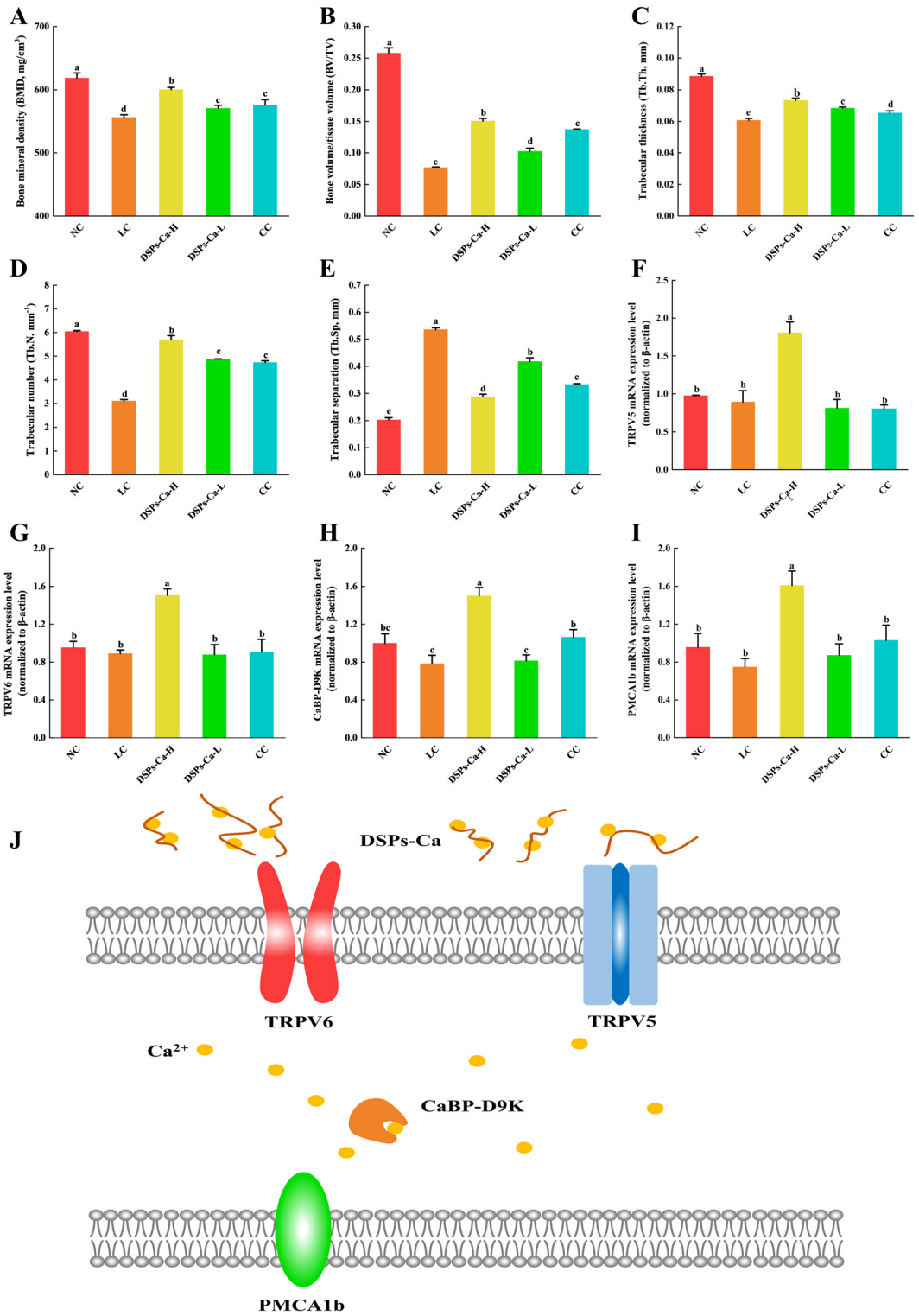

Fig. 7 (A) Bone mineral density (BMD), (B) bone volume/tissue volume (BV/TV), (C) trabecular thickness (Tb.Th), (D) trabecular number (Tb.N), and (E) trabecular separation (Tb.Sp) analyses in each group of mice. Expression of genes responsible for calcium uptake-related genes in the kidneys determined by qRT-PCR. (F) TRPV5; (G) TRPV6; (H) CaBP-D9K; (I) PMAC1b; and (J) possible mechanisms by which DSPs-Ca promote calcium absorption. Different letters indicate significant differences between the groups ($P < 0.05$).

3.14. Gene expression of the corresponding receptors in the kidneys of the mice

Calcium is an important component of bone tissue, and its associated regulatory factors can play a role in bone formation and bone resorption through changes in calcium concentration, and the process of bone metabolism is to a greater extent the process of calcium metabolism.[57] Among them, the regulation of calcium by the kidneys is an important link to calcium metabolism. Calcium uptake in the kidneys can be mediated by the transepithelial calcium channel genes transient receptor potential cation channel subfamily V member 5 and 6 (TRPV5, TRPV6), the calcium-binding protein-D9k (CaBP-D9k) and a calcium pump (plasma membrane Ca-ATPase, PMCA1b) co-mediated. TRPV5 and TRPV6 are important channels for Ca^{2+} transcellular transport, and both of them are distributed in the kidneys. After entering the apical part of epithelial cells through TRPV5 or TRPV6, Ca^{2+} binds to CaBP-D9K and diffuses to the basement membrane, and then calcium ions are transported out of the cell through PMCA1b.[58] We examined the expression of these genes by extracting RNA from the kidney samples from the mice using qRT-PCR, and there were differences in mRNA expression levels in these samples. As shown in Fig. 7F–I, the DSPs-Ca-H group showed significant elevation of the expression of these genes in low-calcium mice compared with the LC group ($P < 0.05$), suggesting that this may be a role of the peptide–calcium chelate. This process may be that DSPs-Ca promotes the ability of related channels to absorb calcium by up-regulating the expression of epithelial calcium channel genes. It is suggested that DSPs-Ca could regulate the opening and mRNA expressions of TRPV5 and TRPV6 channels and regulate calcium ion absorption. Calcium enters and binds to CaBP-D9k. Finally, calcium ions can be released outside the cell *via* PMCA1b (Fig. 7J).

4. Conclusions

Overall, this study utilized Nano LC-MS/MS analysis to measure the amino acid sequences of peptides to provide peptide raw materials with more structural and compositional clarity for the development of peptide–calcium chelate supplements. Structural characterization of deer sinew peptides by SEM, EDS, UV-vis, FTIR, fluorescence spectroscopy, and zeta potential analysis revealed that they combined with Ca^{2+} to form a new substance. Furthermore, DSPs-Ca promoted the proliferation of MC3T3-E1 cells *in vitro* without toxic side effects. Analysis of the *in vivo* studies showed that DSPs-Ca affected serum markers and ameliorated changes in the bone microstructure caused by calcium deficiency, as well as up-regulating the expression of genes responsible for calcium absorption (Trpv5, Trpv6, CaBP-d9k, PMCA1b) in the kidneys. However, this study is limited in exploring chelates for calcium absorption and further of which exact mechanisms are needed in the future. In conclusion, DSPs-Ca could have potential in the development of new calcium supplements.

Abbreviations

DSPs	Deer sinew peptides
DSPs-Ca	Deer sinew peptide-calcium chelate
Micro-CT	Micro-computed tomography
NC	Blank control group
LC	Low-calcium model group
DSPs-Ca-H	Deer sinew peptide-calcium chelate high-dose group
DSPs-Ca-L	Deer sinew peptide-calcium chelate low-dose group
CC	Calcium chloride group

Author contributions

Li Sun: writing—original draft, writing—review and editing, data curation, methodology, validation, investigation, and visualization. Jinze Liu: methodology, investigation and formal analysis. Hongyan Pei: formal analysis and software. Meiling Shi: writing—review and editing. Weijia Chen: supervision and investigation. Ying Zong: conceptualization and validation. Yan Zhao: methodology and investigation. Jianming Li: methodology and validation. Rui Du: conceptualization, funding acquisition, project administration, validation, and writing—review and editing. Zhongmei He: conceptualization, funding acquisition and project administration.

Conflicts of interest

All authors declare that they have no conflict of interest.

Acknowledgements

This work was supported by the Major Science and Technology Project of Sika Deer Industrial Scientific and Technological Innovation—Modern pharmacological connotation, biological mechanism of action and basic research on the traditional core functions of Sika deer medicinal parts (20220304001YY), the Jilin Province Major Science and Technology Special Project (20220304002YY), the Demonstration and Promotion of Sika Deer Breeding and Reproduction, Disease Prevention and Control, Product Processing Industry Technology (202300801-04), the study on key technology and industrialization of deer heart peptide product, a special diet that can increase exercise endurance (23JQ08) and the Jilin Province Science and Technology Department Talent Special—deer sinew chelated calcium preparation key technology and industrialization research (2024086). Icons: Flaticon.com.

References

1 N. Wawrzyniak and J. Suliburska, Nutritional and health factors affecting the bioavailability of calcium: a narrative review, *Nutr. Rev.*, 2021, **79**, 1307–1320.

2 M. Farokhi, F. Mottaghitalab, S. Samani, M. A. Shokrgozar, S. C. Kundu, R. L. Reis, Y. Fatahi and D. L. Kaplan, Silk fibroin/hydroxyapatite composites for bone tissue engineering, *Biotechnol. Adv.*, 2018, **36**, 68–91.
3 R. Bouillon, Nutritional rickets: calcium or vitamin D deficiency?, *Am. J. Clin. Nutr.*, 2021, **114**, 3–4.
4 N. M. Al-Daghri, S. D. Hussain, A. M. Alnaami, N. Aljohani and S. Sabico, Dietary Calcium Intake and Osteoporosis Risk in Arab Adults, *Nutrients*, 2023, **15**, 2829.
5 J. Shlisky, R. Mandlik, S. Askari, S. Abrams, J. M. Belizan, M. W. Bourassa, G. Cormick, A. Driller-Colangelo, F. Gomes, A. Khadilkar, V. Owino, J. M. Pettifor, Z. H. Rana, D. E. Roth and C. Weaver, Calcium deficiency worldwide: prevalence of inadequate intakes and associated health outcomes, *Ann. N.Y. Acad. Sci.*, 2022, **1512**, 10–28.
6 N. Rubio-Lopez, A. Llopis-Gonzalez and M. Morales-Suarez-Varela, Calcium Intake and Nutritional Adequacy in Spanish Children: The ANIVA Study, *Nutrients*, 2017, **9**, 170.
7 J. K. Bird, M. J. Bruins and M. E. Turini, Micronutrient intakes in the Dutch diet: foods, fortified foods and supplements in a cross sectional study, *Eur. J. Nutr.*, 2023, **62**, 3161–3179.
8 K. X. Ye, L. Sun, S. L. Lim, J. L. Li, B. K. Kennedy, A. B. Maier and L. Feng, Adequacy of Nutrient Intake and Malnutrition Risk in Older Adults: Findings from the Diet and Healthy Aging Cohort Study, *Nutrients*, 2023, **15**, 3446.
9 S. Adami, O. Viapiana, D. Gatti, L. Idolazzi and M. Rossini, Relationship between serum parathyroid hormone, vitamin D sufficiency, age, and calcium intake, *Bone*, 2008, **42**, 267–270.
10 B. F. Boyce, Stomaching calcium for bone health, *Nat. Med.*, 2009, **15**, 610–612.
11 C. M. Weaver and M. Peacock, Calcium, *Adv. Nutr.*, 2011, **2**, 290–292.
12 H. A. Bischoff-Ferran, S. Bhasin and J. E. Manson, Preventing Fractures and Falls A Limited Role for Calcium and Vitamin D Supplements?, *JAMA, J. Am. Med. Assoc.*, 2018, **319**, 1552–1553.
13 M. Vavrusova and L. H. Skibsted, Calcium nutrition. Bioavailability and fortification, *LWT–Food Sci. Technol.*, 2014, **59**, 1198–1204.
14 Q. J. Tian, Y. Fan, L. Hao, J. Wang, C. S. Xia, J. F. Wang and H. Hou, A comprehensive review of calcium and ferrous ions chelating peptides: Preparation, structure and transport pathways, *Crit. Rev. Food Sci.*, 2023, **63**, 4418–4430.
15 N. Sun, H. T. Wu, M. Du, Y. Tang, H. W. Liu, Y. H. Fu and B. W. Zhu, Food protein-derived calcium chelating peptides: A review, *Trends Food Sci. Technol.*, 2016, **58**, 140–148.
16 W. J. Qu, Y. H. Li, T. Xiong, Y. H. Feng, H. L. Ma and N. D. K. Akpabli-Tsigbe, Calcium-chelating improved zein peptide stability, cellular uptake, and bioactivity by influencing the structural characterization, *Food Res. Int.*, 2022, **162**, 112033.
17 W. M. Wu, L. C. He, Y. H. Liang, L. L. Yue, W. M. Peng, G. F. Jin and M. H. Ma, Preparation process optimization of pig bone collagen peptide-calcium chelate using response surface methodology and its structural characterization and stability analysis, *Food Chem.*, 2019, **284**, 80–89.
18 S. Chakrabarti, S. Guha and K. Majumder, Food-Derived Bioactive Peptides in Human Health: Challenges and Opportunities, *Nutrients*, 2018, **10**, 1738.
19 J. L. An, Y. X. Zhang, Z. W. Ying, H. Li, W. L. Liu, J. R. Wang and X. Q. Liu, The Formation, Structural Characteristics, Absorption Pathways and Bioavailability of Calcium-Peptide Chelates, *Foods*, 2022, **11**, 2762.
20 H. Zhang, Y. Dong, B. Qi, L. Liu, G. X. Zhou, X. Y. Bai, C. H. Yang, D. Q. Zhao and Y. Zhao, Preventive Effects of Collagen Peptide from Deer Sinew on Bone Loss in Ovariectomized Rats, *Evid.-Based Complement. Altern. Med.*, 2014, **2014**, 627285.
21 H. Zhang, D. A. Pan, Y. Dong, W. J. Su, H. Su, X. H. Wei, C. H. Yang, L. Jing, X. L. Tang, X. Y. Li, D. Q. Zhao, L. W. Sun and B. Qi, Transdermal permeation effect of collagen hydrolysates of deer sinew on mouse skin, ex vitro, and antioxidant activity, increased type I collagen secretion of percutaneous proteins in NIH/3T3 cells, *J. Cosmet. Dermatol.*, 2020, **19**, 519–528.
22 C. T. Wen, D. Wang, Z. Y. Zhang, G. Y. Liu, L. Liang, X. F. Liu, J. X. Zhang, Y. D. Li and X. Xu, Intervention Effects of Deer-Tendon Collagen Hydrolysates on Osteoporosis In Vitro and In Vivo, *Molecules*, 2023, **28**, 6275.
23 Q. Q. Wang, Z. R. Yang, J. C. Zhuang, J. H. Zhang, F. Shen, P. Yu, H. Zhong and F. Q. Feng, Antiaging function of Chinese pond turtle (Chinemys reevesii) peptide through activation of the Nrf2/Keap1 signaling pathway and its structure-activity relationship, *Front. Nutr.*, 2022, **9**, 961922.
24 Y. J. Ning, B. Cui, C. Yuan, Y. Y. Zou, W. Z. Liu and Y. Pan, Effects of konjac glucomannan on the rheological, microstructure and digestibility properties of debranched corn starch, *Food Hydrocolloids*, 2020, **100**, 105342.
25 W. Huang, Y. Q. Lan, W. W. Liao, L. Lin, G. Liu, H. M. Xu, J. P. Xue, B. Y. Guo, Y. Cao and J. Y. Miao, Preparation, characterization and biological activities of egg white peptides-calcium chelate, *LWT–Food Sci. Technol.*, 2021, **149**, 112035.
26 W. J. Qu, Y. T. Feng, T. Xiong, Y. H. Li, H. Wahia and H. L. Ma, Preparation of corn ACE inhibitory peptide-ferrous chelate by dual-frequency ultrasound and its structure and stability analyses, *Ultrason. Sonochem.*, 2022, **83**, 105937.
27 Z. J. Bao, P. L. Zhang, N. Sun and S. Y. Lin, Elucidating the Calcium-Binding Site, Absorption Activities, and Thermal Stability of Egg White Peptide-Calcium Chelate, *Foods*, 2021, **10**, 2565.
28 W. W. Liao, S. J. Liu, X. R. Liu, S. Duan, S. Y. Xiao, Z. N. Yang, Y. Cao and J. Y. Miao, The purification, identification and bioactivity study of a novel calcium-binding peptide from casein hydrolysate, *Food Funct.*, 2019, **10**, 7724–7732.
29 J. Gan, Z. Q. Xiao, K. T. Wang, X. Kong, M. D. Du, Z. H. Wang, B. Xu and Y. Q. Cheng, Isolation, characteriz-

ation, and molecular docking analyses of novel calcium-chelating peptide from soy yogurt and the study of its calcium chelation mechanism, *J. Sci. Food Agric.*, 2023, **103**, 2939–2948.

30 L. Wang, Y. Y. Ding, X. X. Zhang, Y. F. Li, R. Wang, X. H. Luo, Y. N. Li, J. Li and Z. X. Chen, Isolation of a novel calcium-binding peptide from wheat germ protein hydrolysates and the prediction for its mechanism of combination, *Food Chem.*, 2018, **239**, 416–426.

31 W. W. Liao, H. Chen, W. G. Jin, Z. N. Yang, Y. Cao and J. Y. Miao, Three Newly Isolated Calcium-Chelating Peptides from Tilapia Bone Collagen Hydrolysate Enhance Calcium Absorption Activity in Intestinal Caco-2 Cells, *J. Agric. Food Chem.*, 2020, **68**, 2091–2098.

32 W. F. Wu, B. F. Li, H. Hou, H. W. Zhang and X. Zhao, Isolation and identification of calcium-chelating peptides from Pacific cod skin gelatin and their binding properties with calcium, *Food Funct.*, 2017, **8**, 4441–4448.

33 H. Hou, S. K. Wang, X. Zhu, Q. Q. Li, Y. Fan, D. Cheng and B. F. Li, A novel calcium-binding peptide from Antarctic krill protein hydrolysates and identification of binding sites of calcium-peptide complex, *Food Chem.*, 2018, **243**, 389–395.

34 X. Q. Wang, Z. Zhang, H. Y. Xu, X. Y. Li and X. D. Hao, Preparation of sheep bone collagen peptide-calcium chelate using enzymolysis-fermentation methodology and its structural characterization and stability analysis, *RSC Adv.*, 2020, **10**, 11624–11633.

35 L. H. Lao, J. He, W. W. Liao, C. B. Zeng, G. Liu, Y. Cao and J. Y. Miao, Casein calcium-binding peptides: Preparation, characterization, and promotion of calcium uptake in Caco-2 cell monolayers, *Process Biochem.*, 2023, **130**, 78–86.

36 N. Tang and L. H. Skibsted, Calcium Binding to Amino Acids and Small Glycine Peptides in Aqueous Solution: Toward Peptide Design for Better Calcium Bioavailability, *J. Agric. Food Chem.*, 2016, **64**, 4376–4389.

37 D. R. Lin, X. M. Long, L. J. Xiao, Z. J. Wu, H. Chen, Q. Zhang, D. T. Wu, W. Qin and B. S. Xing, Study on the functional properties and structural characteristics of soybean soluble polysaccharides by mixed bacteria fermentation and microwave treatment, *Int. J. Biol. Macromol.*, 2020, **157**, 561–568.

38 H. R. Zhang, L. Y. Zhao, Q. S. Shen, L. W. Qi, S. Jiang, Y. J. Guo, C. H. Zhang and A. Richel, Preparation of cattle bone collagen peptides-calcium chelate and its structural characterization and stability, *LWT–Food Sci. Technol.*, 2021, **144**, 111264.

39 W. Huang, L. H. Lao, Y. L. Deng, Z. W. Li, W. W. Liao, S. Duan, S. Y. Xiao, Y. Cao and J. Y. Miao, Preparation, characterization, and osteogenic activity mechanism of casein phosphopeptide-calcium chelate, *Front. Nutr.*, 2022, **9**, 960228.

40 B. T. Liu, Y. L. Zhuang and L. P. Sun, Identification and characterization of the peptides with calcium-binding capacity from tilapia (Oreochromis niloticus) skin gelatin enzymatic hydrolysates, *J. Food Sci.*, 2020, **85**, 114–122.

41 H. Xiang, H. Huang, D. X. Sun-Waterhouse, X. Hu, L. H. Li, G. I. N. Waterhouse, R. M. Tang, J. Xiong and C. Cui, Enzymatically synthesized gamma-[Glu]((n >= 1))-Gln as novel calcium-binding peptides to deliver calcium with enhanced bioavailability, *Food Chem.*, 2022, **387**, 132918.

42 Z. Y. Wang, S. Z. Cheng, D. Wu, Z. Xu, S. Q. Xu, H. R. Chen and M. Du, Hydrophobic peptides from oyster protein hydrolysates show better zinc-chelating ability, *Food Biosci.*, 2021, **41**, 100985.

43 W. L. Zhai, D. Lin, R. S. Mo, X. Z. Zou, Y. Q. Zhang, L. Y. Zhang and Y. H. Ge, Process Optimization, Structural Characterization, and Calcium Release Rate Evaluation of Mung Bean Peptides-Calcium Chelate, *Foods*, 2023, **12**, 1058.

44 C. Zhang, B. W. Du, Z. H. Song, G. Y. Deng, Y. Shi, T. Y. Li and Y. Q. Huang, Antioxidant activity analysis of collagen peptide-magnesium chelate, *Polym. Test.*, 2023, **117**, 107822.

45 N. Kheeree, K. Kuptawach, S. Puthong, P. Sangtanoo, P. Srimongkol, P. Boonserm, O. Reamtong, K. Choowongkomon and A. Karnchanatat, Discovery of calcium-binding peptides derived from defatted lemon basil seeds with enhanced calcium uptake in human intestinal epithelial cells, Caco-2, *Sci. Rep.*, 2022, **12**, 4659.

46 X. X. Cai, J. P. Lin and S. Y. Wang, Novel Peptide with Specific Calcium-Binding Capacity from Schizochytrium sp Protein Hydrolysates and Calcium Bioavailability in Caco-2 Cells, *Mar. Drugs*, 2017, **15**, 3.

47 Y. L. Lin, X. X. Cai, X. P. Wu, S. N. Lin and S. Y. Wang, Fabrication of snapper fish scales protein hydrolysate-calcium complex and the promotion in calcium cellular uptake, *J. Funct. Foods*, 2020, **65**, 103717.

48 B. Erenay, A. S. Y. Saglam, B. Garipcan, K. D. Jandt and S. Odabas, Bone surface mimicked PDMS membranes stimulate osteoblasts and calcification of bone matrix, *Biomater. Adv.*, 2022, **142**, 213170.

49 S. Z. Deng, A. G. A. Er-bu, H. J. Xie, H. Xiong and B. G. Ye, Evaluation of the acute toxicity and 28-days subacute toxicity of the alcoholic extract from, *Food Sci. Nutr.*, 2023, **11**, 434–442.

50 Y. H. Lee, D. Kim, M. J. Lee, M. J. Kim, H. S. Jang, S. H. Park, J. M. Lee, H. Y. Lee, B. S. Han, W. C. Son, J. H. Seok, J. K. Lee, J. Jeong, J. S. Kang and J. K. Kang, Subchronic toxicity study of Coptidis Rhizoma in rats, *J. Ethnopharmacol.*, 2014, **152**, 457–463.

51 M. D. Zhao, D. U. Ahn, S. M. Li, W. Liu, S. W. Yi and X. Huang, Effects of phosvitin phosphopeptide-Ca complex prepared by efficient enzymatic hydrolysis on calcium absorption and bone deposition of mice, *Food Sci. Hum. Wellness*, 2022, **11**, 1631–1640.

52 N. Carrillo-Lopez, S. Panizo, C. Alonso-Montes, L. Martinez-Arias, N. Avello, P. Sosa, A. S. Dusso, J. B. Cannata-Andia and M. Naves-Diaz, High-serum phosphate and parathyroid hormone distinctly regulate bone loss and vascular calcification in experimental chronic kidney disease, *Nephrol., Dial., Transplant.*, 2019, **34**, 934–941.

53 E. Hernandez-Becerra, D. Jimenez-Mendoza, N. Mutis-Gonzalez, P. Pineda-Gomez, I. Rojas-Molina and M. E. Rodriguez-Garcia, Calcium Deficiency in Diet Decreases the Magnesium Content in Bone and Affects Femur Physicochemical Properties in Growing Rats, *Biol. Trace Elem. Res.*, 2020, **197**, 224–232.

54 M. J. Jia, J. Y. Luo, B. Gao, Y. P. Huangfu, Y. H. Bao, D. H. Li and S. L. Jiang, Preparation of synbiotic milk powder and its effect on calcium absorption and the bone microstructure in calcium deficient mice, *Food Funct.*, 2023, **14**, 3092–3106.

55 K. Nassar and S. Janani, Clinical Risk Factors, Bone Density and Fall's History and Fractures Relation: Study by Hospital Survey About 448 Cases, *Ann. Rheum. Dis.*, 2021, **80**, 1344–1344.

56 K. M. Wiren, X. W. Zhang, D. A. Olson, R. T. Turner and U. T. Iwaniec, Androgen prevents hypogonadal bone loss via inhibition of resorption mediated by mature osteoblasts/osteocytes, *Bone*, 2012, **51**, 835–846.

57 M. K. C. van Goor, J. G. J. Hoenderop and J. van der Wijst, TRP channels in calcium homeostasis: from hormonal control to structure-function relationship of TRPV5 and TRPV6, *Biochim. Biophys. Acta, Mol. Cell Res.*, 2017, **1864**, 883–893.

58 P. P. Hua, Y. Xiong, Z. Y. Yu, B. Liu and L. N. Zhao, Effect of *Chlorella Pyrenoidosa* Protein Hydrolysate-Calcium Chelate on Calcium Absorption Metabolism and Gut Microbiota Composition in Low-Calcium Diet-Fed Rats, *Mar. Drugs*, 2019, **17**, 348.